

## Fragment emission following multiple ionization in 20–200-eV $e^- + \text{H}_2\text{O}$ collisions

F. Frémont, C. Leclercq, A. Hajaji, A. Naja, P. Lemennais, S. Boulbain, V. Broquin, and J.-Y. Chesnel  
*Centre Interdisciplinaire de Recherche Ions Lasers, Unité Mixte CEA-CNRS-EnsiCaen-Université de Caen Basse-Normandie,*  
*6 bd du Mal Juin, F-14050 Caen, Cedex, France*

(Received 27 June 2005; published 3 October 2005)

Collisions between 16–200 eV electrons and  $\text{H}_2\text{O}$  target have been investigated experimentally. The fragment ions originating from single, double, and triple ionization were energetically analyzed at an observation angle of  $90^\circ$  with respect to the incident beam direction. Fragments with energies as low as 0.1 eV were detected. From the spectra, cross sections for double and triple ionization, relative to single ionization cross sections, are derived. The present results are compared with previous experimental results involving several molecular targets, and with formulas that have been developed previously for electron-atom collisions.

DOI: [10.1103/PhysRevA.72.042702](https://doi.org/10.1103/PhysRevA.72.042702)

PACS number(s): 34.80.Gs, 32.80.Hd

### I. INTRODUCTION

Collisions between charged particles and molecules are of great importance in many fields of physics, such as interstellar clouds [1,2], planetary and cometary atmospheres [3], or the effects of radiation damage in biological tissues [4]. For example, in collisions between ions and a cell, it is now recognized that when water is irradiated and ionized, the ejected electrons can have enough kinetic energy to ionize other water molecules. These fast secondary reactions lead to the formation of stable molecules (e.g.,  $\text{H}_2$ ,  $\text{O}_2$ ) and free radicals (e.g., H, OH) and ion species. Thus, a quantitative detailed analysis of the successive processes requires the precise investigation of the different steps of the damage, as, for example, the ionization and fragmentation of  $\text{H}_2\text{O}$  molecules induced by secondary electrons.

In the case of  $e^- + \text{H}_2\text{O}$  collisions, experimental differential [5–7] and total [7–11] cross sections for nondissociative and dissociative single ionization (SI) are now well established, from threshold to impact energies of the order of 10 keV. Models, such as the binary-encounter-dipole (BED) model [12], are shown to provide remarkable methods to predict differential and total ionization cross sections [13–15]. Partial cross sections have also been measured by several groups [8–11,16], with different degrees of precision. For example, differences of a factor of  $\sim 2$  were observed for  $\text{OH}^+$  cross sections and of a factor of  $\sim 4$  for  $\text{H}_2^+$  cross sections [8–11]. Nevertheless, these differences do not affect the total SI cross section since the contributions of  $\text{OH}^+$  and  $\text{H}_2^+$  are small compared to that of  $\text{H}^+$ . Model calculations [17,18] were found to be in reasonable agreement with most of the experiments.

Indirect SI has also been studied for 40 years. Proton kinetic energies from electron impact dissociative ionization of  $\text{H}_2\text{O}$  have been measured by several groups [19–21]. The process of indirect SI requires a double excitation of the molecular target, followed by the ejection of an electron by autoionization. In the following, this process will be referred to as autoionizing double excitation (ADE). According to the authors [21], this process induces fragments whose energies are larger than  $\sim 2$  eV.

The investigation of multiple ionization of  $\text{H}_2\text{O}$  induced by electron impact is rather poor. To our knowledge, only the

case of double ionization (DI) has been previously treated. Concerning the case of DI, only a few articles reported indirect observation of the production of  $\text{H}_2\text{O}^{2+}$  [8,10,11]. From time of flight measurements, Straub *et al.* [11] estimated a cross section for the production of  $\text{H}_2\text{O}^{2+}$  less than  $10^{-20}$  cm<sup>2</sup>, while Rao *et al.* [10] reported observation of  $\text{H}_2\text{O}^{2+}$ , with a measured cross section of  $\sim 10^{-19}$  cm<sup>2</sup> at a projectile energy of 200 eV. In fact, according to Straub *et al.* [11], it is probable that the ions identified as  $\text{H}_2\text{O}^{2+}$  [10] are actually  $\text{O}^{2+}$ . The cross section for the production of  $\text{O}^{2+}$  fragments, measured by Straub *et al.* [11] was estimated to reach a maximum of  $\sim 2 \times 10^{-19}$  cm<sup>2</sup>, in agreement with previous experiments [8]. In addition to the direct DI process, the ejection of two target electrons can be due to the ionization of one inner-shell electron, followed by autoionization. This indirect DI process is efficient for projectile energies larger than  $\sim 32$  eV, corresponding to the binding energy of an electron in the  $2a_1$  orbital of  $\text{H}_2\text{O}$  [22].

Apart from these works, only little is known about the dication states of water. Since the dication bond energies are very low, the dication is unstable and thus quickly dissociates. Some experiments have identified and estimated different ionization potentials of  $\text{H}_2\text{O}^{2+}$ . Using Auger-electron spectroscopy, Moddeman *et al.* [23] measured the lowest DI potential to be 39.4 eV. Richardson *et al.*, by means of photoion-photoion coincidence spectroscopy, measured the lowest DI potential at 36.5 eV [24], corresponding to the dissociation of  $\text{H}_2\text{O}^{2+}$  into the ion pair  $\text{H}^+ + \text{OH}^+$ . This value is  $\sim 3$  eV lower than that reported by Moddeman *et al.* [23], but confirmed by recent measurements [25] using threshold photoelectron coincidence spectroscopy. These results show that the determination of the  $\text{H}_2\text{O}^{2+}$  thresholds remains a challenging task.

In the present work, we investigated the collision  $e^- + \text{H}_2\text{O}$  at projectile energies ranging from 20 to 200 eV. The energy of the fragments emitted after the ionization of  $\text{H}_2\text{O}$  is analyzed at a detection angle of  $90^\circ$ , with respect to the incident beam direction. From the fragment energy distributions, ratios between multiple ionization and SI are determined and compared with previous experimental data related to different molecular targets. Moreover, the present results are compared with two model calculations, developed for ionization of atoms by electron impact.

## II. EXPERIMENTAL SETUP

The experiment has been performed at CIRIL (Caen) using an electron gun of simple design. The beam, collimated to a diameter of  $\sim 1$  mm, was directed to an effusive jet of  $\text{H}_2\text{O}$  molecules. Typical currents of  $\sim 30$  nA at 20 eV and  $\sim 600$  nA at 200 eV were collected in a Faraday cup and were used to normalize the spectra. Ultrapure water (resistivity of  $16.8$  M $\Omega$  cm) purified on an ELGA Maxima System (UFS Elga, France) was used. The fragments produced after the collision were detected using a single-stage electrostatic spectrometer. This spectrometer consists of parallel plates in which a homogeneous electric field is applied. By varying this field, a range of selected ion energies can be explored, giving rise to an energy-distribution spectrum. To obtain total cross section, the experimental doubly-differential cross sections (DDCS) were first integrated with respect to the fragment energy, and then multiplied by  $4\pi$ , assuming that the single-differential cross sections are isotropic. This assumption is realistic, since the projectile does not influence the fragments that are produced after the collision.

## III. FRAGMENT ENERGY DISTRIBUTIONS AND DISCUSSION

### A. Spectra analysis

Figure 1 shows DDCS spectra (circles) for the collision  $e^- + \text{H}_2\text{O}$  as a function of fragment energy per charge, for projectile energies of 20, 35, 37.5, and 200 eV. One should note that the spectrometer selects, for a given electric field, charged particles whose ratios  $E/q$  ( $E$  is the detected fragment energy and  $q$  the charge) are identical. To make easier the forthcoming analysis, the experimental DDCS were fitted using Gaussian curves (dashed curves in Fig. 1). The full curve represents the sum of the Gaussian curves. The position of the different Gaussian peaks was determined in order to reproduce as well as possible the experimental data. In addition, consistently with the instrumental energy resolution, the width of the Gaussian curves was chosen to be proportional to their mean energy. The quality of the fitting procedure was verified by means of the  $\chi^2$  value.

At 20 eV (top of Fig. 1), a structure (labeled b) centered at  $\sim 0.2$  eV dominates, while a shoulder (a) at energies smaller than 0.15 eV appears. According to the previous measurements [9–11,22], the peak (b) is attributed to  $\text{H}^+$  fragments in the  $\text{H}^+ + \text{OH}$  channel. The unambiguous assignment of the dominant peak allowed us to normalize our data with other experimental cross sections [11]. The small contribution (a) can be due to the emergence of  $\text{O}^+$  fragments. This observation is confirmed by Rao *et al.* [10] who found a threshold for these fragments at  $\sim 20$  eV. At 20 eV, the authors found a ratio  $\sigma(\text{H}^+)/\sigma(\text{O}^+)$  of  $\sim 6$ , where  $\sigma(\text{H}^+)$  and  $\sigma(\text{O}^+)$  are partial cross sections for the production of  $\text{H}^+$  and  $\text{O}^+$  fragments, respectively. This ratio is, within the experimental uncertainties, in agreement with the ratio of  $\sim 9$  in the present work.

At a projectile energy of 35 eV, structures (a) and (b) still exist, and are found to increase in intensity by a factor of  $\sim 30$ . Two additional structures labeled (c) and (d) in Fig. 1

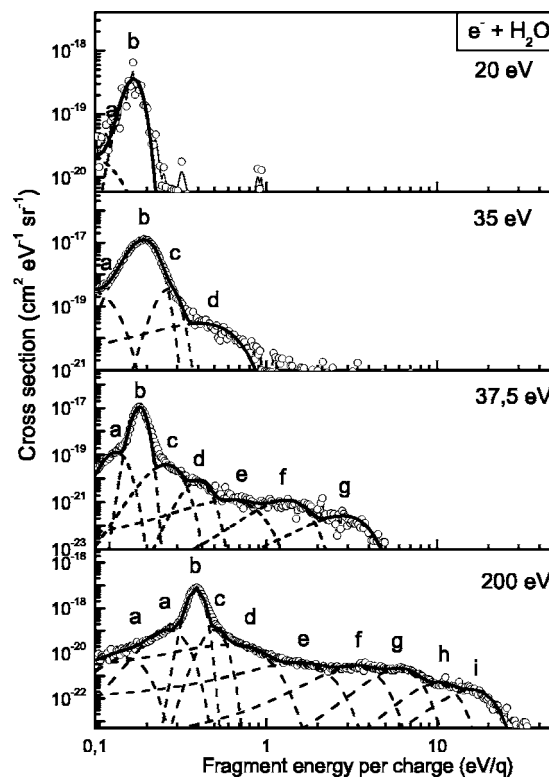


FIG. 1. Energy distributions of fragments following ionization of  $\text{H}_2\text{O}$  molecules after electron impact at projectile energies of 20, 35, 37.5, and 200 eV, for an observation angle of  $90^\circ$ . a–b: single ionization; c–g: indirect and direct double ionization; h, i: triple ionization. The Gaussian curves (dashed curves) are used to fit the experimental spectra.

are located at around 0.3 and 0.5 eV. The origin of these structures is not straightforward, since no calculation is available. Nevertheless, from previous experiments [24], one can make some remarks. It is established that the kinetic energy release of the pairs  $\text{H}^+ + \text{OH}^+$  and  $\text{H}^+ + \text{O}^+$  are of the order of 4.5 and 5 eV, respectively [24]. Thus, the energy of a  $\text{H}^+$  fragment is close to  $\sim 4$  eV for both channels. Since no structure is visible at these energies, the contribution of the direct DI is negligible. In addition, it is seen that no peak appears at energy higher than 2 eV, indicating that the contribution of ADE is negligible.

To explain the emergence of the additional structures (c) and (d), it is recalled that, at a projectile energy of 35 eV, an inner-shell electron from the  $2a_1$  orbital may be ionized, as mentioned in the Introduction. Then, after the collision, the  $\text{H}_2\text{O}^+$  residual target may autoionize. When such low lying electrons are involved in the production of a vacancy, the time required by the Auger process is typically of the order of  $10^{-12}$  s, which is much longer than the dissociation time ( $\sim 10^{-14}$  s). Hence, the autoionization process occurs after the dissociation of  $\text{H}_2\text{O}^+$ , so that it is reasonable to expect a  $\text{H}^+$  fragment energy close to the energy of a  $\text{H}^+$  fragment when an outer-shell electron is ionized. These observations have also been made in the case of double photoionization of  $\text{H}_2\text{S}$  below the double ionization threshold [26,27]. The present experiment indicates that the DI threshold for  $\text{H}_2\text{O}$  is  $\sim 35$  eV or less.

As the projectile energy increases (37.5 and 200 eV), the spectra reveal additional structures. At 37.5 eV, the fragment energies reach values of  $\sim 5$  eV, suggesting an increase of the target excitation. At 200 eV projectile energy, fragments whose energies are as high as 30 eV are observed. At the latter projectile energy, two structures [labeled (h) and (i) on bottom of Fig. 1] are centered at energies larger than 10 eV. According to a previous experiment involving highly charged ions as projectiles [28], these structures can be attributed to  $H^+$  fragments after the formation of  $H_2O^{3+}$ . In the present experiment, the structures due to TI appear at projectile energies of at least 75 eV. This result provides a first estimate of the TI threshold.

Finally, Fig. 1 shows that the mean energy of the structure (b) increases when increasing the projectile energy. At low energy, this structure is peaked at  $\sim 0.17$  eV and reaches 0.34 eV at 200 eV. This finding is consistent with the result of Tan *et al.* [22] who found  $H^+$  kinetic energies of 0.14 and 0.34 eV at photon energies of 25 and 50 eV, respectively. According to the authors, the shift in energy is due to the increasing degree of excitation of the molecule.

### B. Multiple ionization cross sections

Despite the lack of exact assignment of the different structures in the fragment spectra, the above discussion allows for the determination of at least a *maximum* value for the multiple ionization cross sections. From our experiment, the maximum value for DI (resp. for TI) is determined by integration of the structures labeled (c) to (g) [resp. (h) and (i)]. On the other hand, integration of peak (b) leads to the cross section  $\sigma(H^+)$  for emission of  $H^+$  fragments induced by dissociative SI. Thus, the present experiment provides ratios  $\sigma_q/\sigma(H^+)$ , where  $\sigma_q$  is an upper limit of the cross section for the ejection of  $q$  electrons from the target. Then, by using the total SI cross section  $\sigma_1$  and the cross section  $\sigma(H^+)$  available in the literature [7,11], it is possible to deduce the maximum values for the ratios  $\sigma_q/\sigma_1$  of multiple ionization over SI. The results are presented in Fig. 2 for  $q=2$  and 3, as a function of the projectile energy. The ratios are found to increase with the projectile energy by a factor of  $\sim 10$  in the range 35–200 eV. The ratio  $\sigma_2/\sigma_1$  is  $\sim 10^{-3}$  at 35 eV and reaches  $\sim 1\%$  at 200 eV, while the ratio  $\sigma_3/\sigma_1$  is about one order of magnitude smaller.

The present ratios can be compared with those obtained for several molecular targets. In Fig. 2, we reported the ratios for HCl [29],  $N_2$ , and  $O_2$  targets [30]. Since double and triple ionization thresholds for these molecules are rather close to those for  $H_2O$  (Table I), the ratios are expected to be of the same order of magnitude. First, we consider the ratio  $\sigma_2/\sigma_1$  (left side of Fig. 2). The ratio  $\sigma_2/\sigma_1$  for  $H_2O$  is found to be significantly smaller than that for HCl,  $N_2$  and  $O_2$ , especially at high projectile energies. For instance, at impact energies larger than 100 eV, the ratio  $\sigma_2/\sigma_1$  is about the same (within a factor of 2) for HCl,  $N_2$ , and  $O_2$ , while it is surprisingly 5 to 10 times lower for  $H_2O$ . In contrast, the TI ratios  $\sigma_3/\sigma_1$  for  $H_2O$  is found to be about the same as that for the other

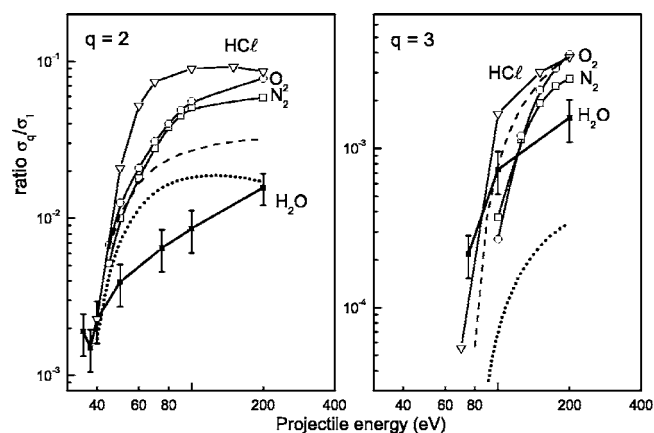


FIG. 2. Cross section  $\sigma_q$  for the ionization of  $q$  electrons ( $q=2,3$ ) from  $H_2O$  (full squares) relative to single ionization cross section  $\sigma_1$ . The present results are compared with those obtained for several molecular targets and simple formula. Experiment:  $\circ$ ,  $N_2$ ;  $\square$ ,  $O_2$ ;  $\nabla$ , HC. The dashed curves and the dotted curves are derived from the semiempirical Bethe-Born type formula by Shevelko and Tawara [31], and from the scaling law by Fisher *et al.* [15].

molecules (right side of Fig. 2). The large difference observed for  $\sigma_2/\sigma_1$  might be due to an underestimation of our cross section ratios. However, we note that the finding of a smaller probability to remove two electrons in the case of  $H_2O$  is consistent with the lower number of available electrons in  $H_2O$  compared to that for HCl,  $N_2$ , and  $O_2$ . From the experimental data, it is clear that the cross sections for multiple ionization of molecular targets cannot be easily predicted by comparing results obtained with different molecules. Precise calculations are thus needed for a better understanding of the multiple ionization processes occurring in collisions between charged particles and molecules.

Since such calculations are not available for electron molecule collisions, we used simple formulas that have been obtained in the case of electron-atom collisions [15,31]. In Fig. 2 the ratios derived from the semiempirical Bethe-Born-type formula by Shevelko and Tawara [31] (dashed curves) and from the scaling law by Fisher *et al.* [15] (dotted curves) are presented. For DI, the agreement is reasonable, since the differences between calculation and experimental results do not exceed a factor of 3. In the case of TI process, the scaling law and the experiment give similar ratio, within a factor of  $\sim 2$ , while the Bethe-Born type formula induces a strong difference with the experiment by a factor of  $\sim 5$  at high

TABLE I. Single-, double-, and triple-ionization thresholds (eV) for  $H_2O$ , HC [29],  $N_2$  and  $O_2$  [30] molecules.

Molecules	Thresholds (eV)		
	SI	DI	TI
$H_2O$	15	35	75
HC	12.7	35.5	70
$N_2$	20	45	100
$O_2$	17.5	45	100

projectile energies. These results clearly show that specific calculations are needed, taking into account both direct and indirect processes for the formation of fragments.

#### IV. CONCLUSION

The fragmentation of H<sub>2</sub>O induced by electron impact has been investigated by means of ion spectroscopy, at projectile energies ranging from 16 to 200 eV. At projectile energies smaller than 35 eV, the SI process dominates. When the projectile energy increases, structures associated with indirect and direct DI appear. The DI threshold was found to be of the order of 35 eV. The fragments originating from indirect DI are produced by a SI involving inner-shell electrons, followed by autoionization of the residual H<sub>2</sub>O<sup>+</sup> target before it dissociates. At projectile energies larger than 75 eV, a struc-

ture, associated with TI, is evidenced at fragment energies of ~16 eV. By integration in energy of individual Gaussian curves which were used to fit the experiment, we could determine the cross sections for ionization of 2 and 3 target electrons, relative to SI cross sections, as a function of the projectile energy. The present results were compared with those obtained for several molecular targets, and also with simple formula that have been developed for electron-atom collisions. Unexpectedly, the ratio between DI and SI for H<sub>2</sub>O is found to be much smaller than that for the other molecules. The comparison with results derived from simple formula shows a rather good overall agreement. A complete calculation, taking into account direct as well as indirect processes, would be desirable to confirm our measured cross sections, and to allow for a better understanding of the multiple ionization processes as well.

- 
- [1] E. Herbst, *Annu. Rev. Phys. Chem.* **46**, 27 (1995).  
 [2] J. Black, *Faraday Discuss.* **109**, 257 (1998).  
 [3] B. G. Lindsay, *J. Geophys. Res.* **109**, A08305 (2004).  
 [4] B. Boudaiffa, P. Cloutier, D. Hunting, M. A. Hues, and L. Sanche, *Science* **287**, 1658 (2000).  
 [5] C. B. Opal, W. K. Peterson, and E. C. Beaty, *J. Chem. Phys.* **55**, 4100 (1971).  
 [6] D. A. Vroom and R. L. Palmer, *J. Chem. Phys.* **66**, 3720 (1977).  
 [7] M. A. Bolarisadeh and M. E. Rudd, *Phys. Rev. A* **33**, 882 (1986).  
 [8] J. Schutten, F. J. de Heer, H. R. Moustapha, A. J. H. Boerboom, and J. Kistenmaker, *J. Chem. Phys.* **44**, 3924 (1966).  
 [9] O. J. Orient and S. K. Srivastava, *J. Phys. B* **20**, 3923 (1987).  
 [10] M. V. V. S. Rao, I. Iga, and S. K. Srivastava, *J. Geophys. Res.* **100**, 26421 (1995).  
 [11] H. C. Straub, B. G. Lindsay, K. A. Smith, and R. F. Stebbings, *J. Chem. Phys.* **108**, 109 (1998).  
 [12] Y.-K. Kim and M. E. Rudd, *Phys. Rev. A* **50**, 3954 (1994).  
 [13] M. Gryzinski, *Phys. Rev.* **138**, A322 (1965).  
 [14] L. Vriens, *Proc. Phys. Soc. London* **89**, 13 (1966).  
 [15] V. Fisher, Y. Ralchenko, A. Goldgirsh, D. Fisher, and Y. Maron, *J. Phys. B* **28**, 3027 (1995).  
 [16] J. C. Gomet, *C. R. Seances Acad. Sci., Ser. B* **281**, 627 (1975).  
 [17] S. P. Khare and W. J. Meath, *J. Phys. B* **20**, 2101 (1987).  
 [18] S. P. Khare, S. Prakash, and W. J. Meath, *Int. J. Mass Spectrom. Ion Process.* **88**, 299 (1989).  
 [19] H. Ehrhardt and A. Kresling, *Z. Naturforsch. A* **22a**, 2036 (1967).  
 [20] J. Appel and J. Durup, *Int. J. Mass Spectrom. Ion Phys.* **10**, 247 (1972).  
 [21] R. B. Cordaro, K. C. Hsieh, and L. C. McIntyre, *J. Phys. B* **19**, 1863 (1986).  
 [22] K. H. Tan, C. E. Brion, P. E. Van der Leeuw, and M. J. Van der Wiel, *Chem. Phys.* **29**, 299 (1978).  
 [23] W. E. Moddeman, T. A. Carlson, M. O. Krause, B. P. Pullen, W. E. Bull, and G. K. Schweiter, *J. Chem. Phys.* **55**, 2317 (1971).  
 [24] P. I. Richardson, J. H. D. Eland, P. G. Fournier, and D. L. Cooper, *J. Chem. Phys.* **84**, 3189 (1986).  
 [25] S. J. Cavanagh, S. Y. Truong, P. Bolognesi, and G. C. King, *Sci Rep SRS, Atomic Mol. Spectro.* 2 (2000).  
 [26] J. H. D. Eland, P. Lablanquie, M. Lavollée, M. Simon, R. I. Hall, M. Hochlaf, and F. Penent, *J. Phys. B* **30**, 2177 (1997).  
 [27] K. F. Dunn, R. Browning, M. A. MacDonald, C. R. Browne, and C. J. Latimer, *J. Phys. B* **31**, 4173 (1998).  
 [28] B. Siegmann, U. Werner, H. O. Lutz, and R. Mann, *J. Phys. B* **34**, L587 (2001).  
 [29] S. Harper, P. Calandra, and S. D. Price, *Phys. Chem. Chem. Phys.* **3**, 741 (2001).  
 [30] C. Tian and C. R. Vidal, *J. Phys. B* **31**, 5369 (1998).  
 [31] V. P. Shevelko and H. Tawara, *Atomic Multielectron Processes* (Springer-Verlag, Berlin, 1998).